IEEE Access
Multidisciplinary | Rapid Review | Open Access Journal

Received September 22, 2020, accepted October 14, 2020, date of publication October 19, 2020, date of current version October 28, 2020.

Digital Object Identifier 10.1109/ACCESS.2020.3032065

Design Analysis and Evaluation of a W-Element Model for a Twisted-Pair Cable

MOHAMMAD ZAREI, (Member, IEEE), AMIN KHALILZADEGAN, (Member, IEEE), AND KHAYROLLAH HADIDI, (Member, IEEE)
Microelectronics Research Laboratory, Urmia University, Urmia 5756151818, Iran
Corresponding author: Mohammad Zarei (m.zarei@urmia.ac.ir)

ABSTRACT Unlike the twisted pair cable's simple installation mechanism, evaluating a circuit equivalent and certifying it is not very convenient anymore. Although the best way to model transmission lines is to use the field solver software programs such as ANSYS Maxwell or HFSS, this procedure is very overwhelming and time-consuming. This paper presents a straightforward approach to extract a W-element model for the twisted pair cable based on its structural and electrical characteristics. The W-element model employs a novel state-of-the-art transmission line simulation method which is very fast, accurate and robust. Both system designers and cable manufacturers can easily exploit the presented equations and the derived models to predict the behavior of the balanced transmission lines with two conductors using simulators such as HSpice, etc. Nexans unshielded CAT6 twisted pair cable, one of the most common types of cables used in today's networks, is selected as a case study in this paper to verify the proposed model. A variety of simulations have been carried out to evaluate the performance and accuracy of the proposed model. Furthermore, the validity of the model is assessed against the real Fluke test results.

INDEX TERMS Twisted pair cable, W-element, transmission line modeling, fluke test, RLGC model.

NOMENCLATURE

ε_0	Permittivity of free space
ε_r	Relative permittivity of material
μ_0	Magnetic permeability of free space
μ_r	Relative magnetic permeability of material
ρ	Specific electrical resistance of material
σ	DC conductivity of the insulation material
δ	Skin depth
f	Frequency
d	Diameter of the conductor
D	Center to center separation of the conductors
H	Height of the wire above the ground
NVP	Nominal Velocity of Propagation
$\tan(\delta)$	Loss tangent of insulation material
k_p	Correction factor of proximity effect
l	Length of wire
l_{max}	Maximum length of RLGC element
L_{Cable}	Cable jacket length
L_{wire}	Wire's electrical length
$L_{wire-pitch}$	Wire's pitch length
R_{Pitch}	Pitch radius of twisted pair
R	Series resistance of RLGC element
L	Series inductance of RLGC element
G	Shunt conductance of RLGC element
C	Shunt capacitance of RLGC element
R_{DC}	DC resistance matrix of W-element
R_{AC}	AC resistance matrix of W-element
L_0	DC inductance matrix of W-element
G_0	DC Dielectric-loss matrix of W-element
G_d	AC Dielectric-loss matrix of W-element
C_0	DC capacitance of conductor of W-element
R_0	DC resistance of conductor
R_{SP}	Skin-effect resistance of conductor
L_S	Self-inductance of conductor
M	Mutual inductances of conductors
G_{dm}	Dielectric loss of the insulation material
C_S	Self-capacitance of conductor
C_M	Mutual capacitance of conductors

The associate editor coordinating the review of this manuscript and approving it for publication was Wei-Wen Hu.

I. INTRODUCTION

Nowadays, the data rate of digital systems has been increased at a quick pace so that the effect of the communication mediums must be modeled and involved in the design process [1]–[3]. When the frequency reaches several hundreds of megahertz, the communication medium is no longer a simple

conductor and acts like a transmission line [4]. Accordingly, system designers are eager to gain rapid and clear insight into how far and fast data moves over the communication medium prior to fabrication [5]–[7]. Besides, cable manufacturers are really interested in finding out how the performance of the designed cable is altered by changing its characteristics. Although the best way to model transmission lines is to use field solver software programs such as ANSYS Maxwell or HFSS [8], this procedure is very overwhelming and time-consuming. Therefore, a set of closed-form and straightforward equations which relate the behavior of the cable to its dimension, material and operating frequency; or an electrical equivalent circuit that is used by a simulator to evaluate voltage and current waveforms in the circuit, will be very useful for both system designers and cable manufacturers [9].

The transmission medium can take a variety of forms [10]. Among all forms, twisted pair cables are widely exploited in the diversity of the electronic systems owing to their prominent characteristics and lower cost [1], [2]. Modeling of the twisted pair cables was thoroughly investigated in the literature. Some models have been extracted experimentally based on the S-parameter [11]–[16] or time-domain measurements [17]–[25]. The main disadvantage of the experimental models is that all measurements must be repeated even only by changing one of the cable parameters. Also, measurement errors will affect the accuracy of these models. In addition to these models, some theoretical researches and mathematical calculations have been done to model twisted pair cables [26]–[29]. Despite many research efforts made for modeling twisted pair cables, there is no straightforward model to be exploited in circuit simulation software programs like HSpice. Hence, developing a family of closed-form formulas for full-fledged modeling of twisted-pair cables in terms of its characteristics is the main motivation of this research. In this paper, a set of straightforward closed-form formulas is presented to calculate the W-element model's parameters of any twisted pair cable by considering several important factors such as material and structural make-ups, twist pitch, skin effect, proximity effect, etc. In this way, there is no need for further complicated and time wasting approaches such as sketching new design model in field solver software or doing test experiments. It is enough to place the new value of the parameters in the proposed equation to obtain the model. Since the proposed methodology is a general purpose one, it can be easily applied to a wide variety of cable types like shielded twisted pair. The important point that should be bear in mind is that the calculation of some parameters like self-capacitance will vary in the presence of the shielding material.

The rest of this paper is organized as follows: Section 3 argues about lumped and distributed modeling of the transmission medium. Section 4 introduces the W-element as a versatile tool for modeling diversity of transmission line structures, from a simple lossless line to complex frequency-dependent lossy-coupled lines. In Section 5, different characteristics of twisted pair cable are parameterized and a set of closed-form formula is provided for its modeling. In order to evaluate the performance of the derived formulas, the accuracy of the CAT6 twisted-pair model is validated against real Fluke test results and HFSS simulations, as a case study in Section 6. Finally, concluding remarks are provided in Section 7.

II. LUMPED VERSUS DISTRIBUTED MODEL OF TRANSMISSION MEDIUM

In the case that the signal frequency is low and the physical dimension of the transmission medium is such that the level of the signal is reasonably constant along its entire length, the transmission medium can be safely modeled by a set of lumped elements [2]. This model works successfully in low frequencies but falls apart at high frequencies. In other words, by increasing the frequency, the transmission medium should no longer be considered as a simple lumped-element and must be treated in a distributed form [4]. Based on the telegrapher's equations, the efficient way to model a transmission line is by breaking it into a series of two-port cascaded lumped segments and then using the two-port analysis to predict the overall behavior of the system as is shown in Fig. 1. In general, the telegrapher's equations are applicable to any transmission media like twisted pair cable which has the following properties [30]:

- At least two conductors, insulated from each other,
- Having a uniform cross-section along the entire length of the structure,
- With a small cross-sectional geometry compared to the wavelength of the signals conveyed, and
- A long length compared to the spacing between the conductors.

It is noted that the length of individual segments must be relatively small with respect to the transmitted wavelength over the transmission line [3]. Each segment is modeled by four RLGC components, as shown in Fig. 2. Values of R, L, G, and C represent the cumulative amount of resistance, inductance, capacitance and conductance for the entire length of specified segments. The values of these parameters are affected not only by the geometry of the transmission line but also by the electrical characteristics of the dielectric and conductors [31]. Series resistance (R) and shunt conductance (G) are included due to the conductors' finite conductivity and dielectric loss of the material between them, respectively. The total self-inductance of the conductors is modeled by a series inductance (L) and a shunt capacitance (C) is added owing to the proximity of the two conductors [1]. Although the dominant factors are L and C, both R and G must be calculated precisely and taken into account to increase the transmission line model's accuracy.

It should be kept in mind that choosing the right length or number of the lump segments along the transmission line is very important in the modeling procedure. Although choosing a too small length for each lumped section increases the accuracy of the modeling, it does not have an obvious effect

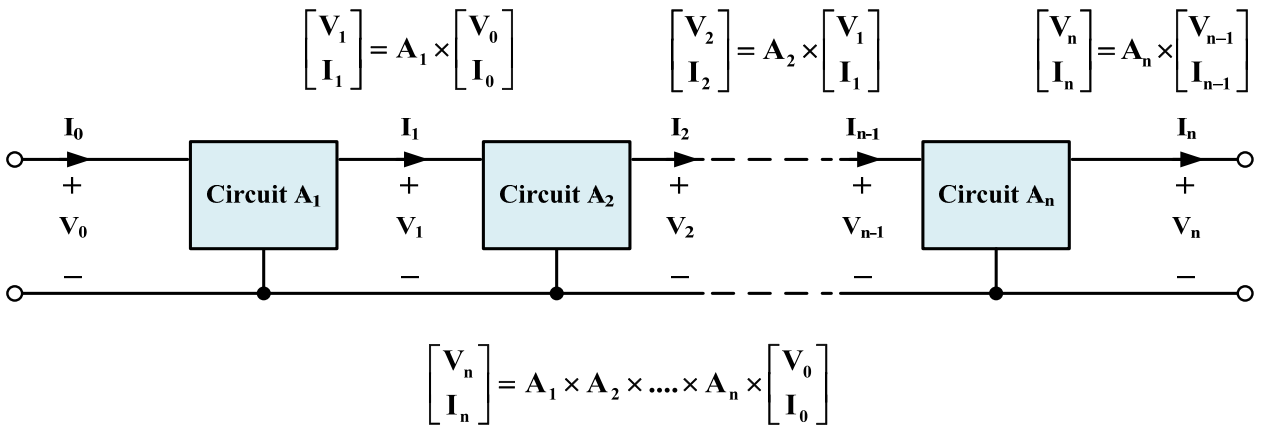

FIGURE 1. Modeling of transmission line using series of cascaded two-port circuits.

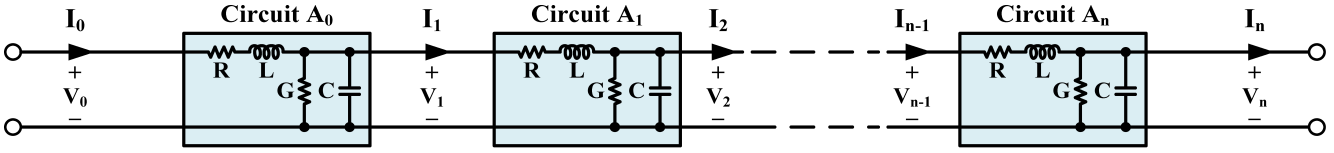

FIGURE 2. Modeling of transmission line using series of cascaded RLGC segments.

on the accuracy of results and just increases the simulation time [32].

In the case of a sinusoidal signal being transmitted, there is a general agreement that if the interconnect line length is less than one-twentieth of the signal wavelength, it can be model as a simple lumped RLGC element [33]. Similarly, the maximum length (l_{max}) constraint for a pulse shaped signal is obtained in the form of (1):

$$l_{\max} = 0.2\mathrm{t_r}.\mathrm{NVP} \tag{1}$$

where t_r and NVP are the rise time and propagation speed of the pulsed signal, respectively. NVP stands for nominal velocity of propagation and represents the speed at which the data signals travel through the cable and is announced by the cable manufacturers. Usually, this parameter is expressed as a percentage of the speed of light in vacuum [34].

III. W-ELEMENT MODEL

W-element employs a novel state-of-the-art transmission line simulation method which is very fast, accurate and robust. The diversity of the transmission lines can be modeled in HSPICE using the W-element based on the distributed RLGC matrices. This approach is very general and applicable for most interconnect systems, due to the ability to represent any number of coupled interconnects, and the ability to handle substantial-frequency dependencies [31], [35].

R_0 (DC resistance), L_0 (DC inductance), G_0 (DC shunt conductance), C_0 (DC capacitance), R_s (skin-effect resistance), and G_d (dielectric-loss conductance) matrices are the inputs for each W-element model [34]. Since W-element is used to model both loss-less and lossy transmission lines, L_0 and C_0 are the essential parts of all models. The other parameters are optional and may be omitted for some cases. If one of the optional parameters is specified, all preceding parameters have to be specified even if they are zero [21]. In general form, the dimension of these matrices for a transmission line with N number of signal conductors would be N × N. Since these matrices are symmetrical about their main diagonal, it is enough to specify only the lower triangular elements of them. Accordingly, for transmission lines like twisted pair cable with two signal conductors; dimension of matrices would be 2 × 2 and only 3 different elements need to be determined.

A. RESISTANCE MATRICES

The Resistivity of a material is a measure of how it resists against an electric current flow through it. Since the current distribution in the cross-sectional area of a conductor varies by altering the frequency, resistive behavior of the transmission lines cannot be modeled only with simple constant resistors [5]. This phenomenon squeezes the current into a shallow region just underneath the surface of the conductor and increases the apparent resistance called the skin effect. Furthermore, the current distribution of the conductor and consequently the value of its resistance is also affected by the magnetic field of adjacent conductors due to proximity effect [6]. Therefore, the resistance of the transmission line has to be expressed by DC (R_{DC}) and AC (R_{AC}) matrices based on (2).

$$\mathrm{R_{Transmissionline}} = \mathrm{R_{DC}} + \mathrm{R_{AC}}\sqrt{f} \tag{2}$$

Since conductors do not affect each other at DC frequencies, so R_{DC} matrix is in the diagonal form. Although two nearby conductors affect each other due proximity effect and this issue has to be modeled in terms of off-diagonal elements, AC resistance matrix can be modeled as a diagonal matrix. The details of this argument will be discussed in the following section. Consequently, R_{DC} and R_{AC} matrices come in the following form.

$$R_{DC} = \begin{bmatrix} R_0 & 0 \\ 0 & R_0 \end{bmatrix} \tag{3}$$

$$R_{DC} = \begin{bmatrix} R_{SP} & 0 \\ 0 & R_{SP} \end{bmatrix} \tag{4}$$

In the above equations, R_0 is the DC resistance of the conductors which is simply obtained by a simple resistivity equation and R_{SP} represents how the resistance of the conductors alters by increasing frequency due to the skin and proximity effect.

B. DC INDUCTANCE MATRIX

It is obvious that any conductor which carries a time-varying current, produces magnetic flux around itself and therefore a voltage is induced on it. This issue can be modeled by a series inductance. In the DC inductance matrix of the transmission line, the main diagonal terms are equal to self-inductance of the conductors (L_S), while the off-diagonal terms are equal to mutual inductances between them (M). The general form of this matrix is shown in (5).

$$L_0 = \begin{bmatrix} L_S & M \\ M & L_S \end{bmatrix} \tag{5}$$

C. DC CAPACITANCE MATRIX

Since there is a potential difference between the conductors of the transmission lines, a capacitance exists. The conductors of the transmission line and insulation between them act as plates of capacitance and dielectric material, respectively.

DC capacitance matrix of the W-element model is in the Maxwellian format [36] which means that the main diagonal terms of this matrix are the sum of all self and mutual components that are connected to the corresponding conductor with signs intact. Besides, the off-diagonal terms are equal to the mutual capacitance that exists between two conductors by a negative sign. For more clarification, consider a transmission line with two conductors, namely T_1 and T_2, as shown in Fig. 3 for determining the DC capacitance matrix.

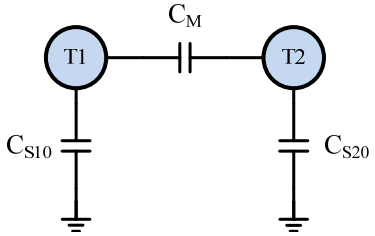

FIGURE 3. Self and mutual capacitance of the transmission line.

C_S and C_M in Fig. 3 are the self and mutual capacitances, respectively. With given assumptions, the DC capacitance matrix comes in the form of (6). Due to the symmetry of the structure, the self-capacitance of both wires, namely C_{S10} and C_{S20}, is the same and is denoted by C_S.

$$C_0 = \begin{bmatrix} C_S + C_M & -C_M \\ -C_M & C_S + C_M \end{bmatrix} \tag{6}$$

D. SHUNT CONDUCTANCE MATRIX

DC conduction and high-frequency dipole relaxation are the important factors that lead to some energy loss in the dielectric material of the transmission lines. Although the impact of the dielectric loss can be ignored for most of the practical applications, it must be considered in the model for more accuracy. In general, total dielectric loss is described by (7) [31]:

$$G_{\text{Transmission line}} = G_0 + f \cdot G_d \tag{7}$$

where G_0 and G_d are the DC and AC dielectric loss matrices, respectively. Due to the small value of the DC conductivity of the insulation materials (σ), the dielectric loss can be ignored for DC frequencies or $G_0 = 0$. By doing so, the DC conductance matrix would be null. By increasing the frequency, dielectric loss also increases owing to further absorption of electrical energy by insulation material. Similar to the DC capacitance matrix, the dielectric-loss conductance matrix is also in the Maxwellian format. By ignoring the dielectric loss between conductors and ground plane, G_d matrix comes in the form of (8):

$$G_d = \begin{bmatrix} G_{dm} & -G_{dm} \\ -G_{dm} & G_{dm} \end{bmatrix} \tag{8}$$

where G_{dm} is the dielectric loss of the insulation material between conductors.

IV. W-ELEMENT MODEL OF TWISTED PAIR CABLE

Twisted pair cable is the most common form of the transmission medium for modern data communication applications [9]. It is simply composed of four-wire pairs (8 wires) in a cable sheath. Every wire is coated with some type of insulating material such as a paper-based or a plastic-based material. Since the wires of each pair are physically close and symmetrically intertwined together, any outside influence will affect them similarly and therefore, its effect is canceled out when differential voltage is applied to the wires [1]. If the twist rate of all pairs is equal, the same conductors of the adjacent pairs may repeatedly lie next to each other and lead to crosstalk increasing between them. Hence, twisting rates of pairs are considered different with respect to each other for further reducing crosstalk [6], [21]. Twisted pair cables are classified into several categories based on their characteristics [37]. Since unshielded CAT6 twisted pair (UTP CAT6) cable is the best candidate in most of today's networks by taking into account all of its pros and cons, the W-element model of this type of twisted pair cable is extracted to evaluate the validity of the presented model in the following section.

However, the algorithm of W-elements does not have any hard frequency limitations. The frequency range of applicability of W-element is limited essentially by the range of applicability of the corresponding transmission line, and by the accuracy of the frequency-dependent RLGC parameters provided by the W-element model [38]. The cable that is selected as a case study in the manuscript supports all applications up to 250 MHz and the proposed model is applicable in this frequency range.

A. CABLE LENGTH VERSUS WIRE LENGTH

In order to model a twisted pair cable, its geometries must be parameterized first of all. Fig. 4 (a) and (b) show the structure and geometry of the twisted pair cable, respectively.

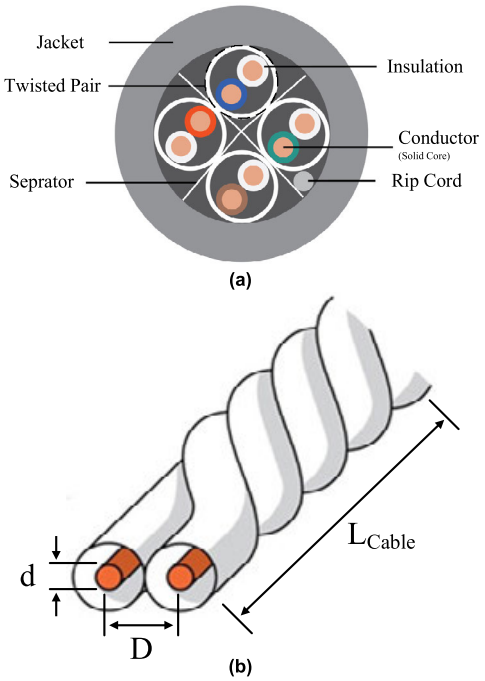

FIGURE 4. (a) Structure (b) geometries of twisted pair cable.

According to Fig. 4 (b), the diameter of conductors and separation distance between them is denoted by d and D, sequentially. Since the wires inside the cable are in helical form, their actual (electrical) length is greater than the length of the cable jacket [39]. To differentiate them, cable jacket length and wire electrical length are denoted by L_{Cable} and L_{wire}, respectively. These two parameters are related together via the wire's pitch length value ($L_{wire-pitch}$). Pitch length is defined as the axial distance required in which a wire completes one revolution around the diameter of the other conductor and returns to its original relative position in a twisted pair cable, as is shown in Fig. 5. The pitch radius for twisted pair cable (R_{Pitch}) equals half of the center to center separation of the conductors (D).

It is obvious from Fig. 5 that the real length of the wire for one pitch of the twisted pair can be easily extracted by

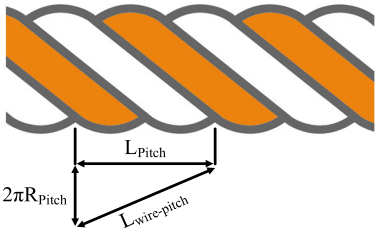

FIGURE 5. Pitch length of twisted pair cable.

applying the well-known Pythagorean Theorem as following:

$$L_{wire-pitch} = \sqrt{L_{Pitch}^2 + \pi^2 D^2} \tag{9}$$

Knowing that the number of pitches along the twisted pair derives simply by dividing L_{Cable} by L_{Pitch}, the total wire length relates to the cable geometries based on the (10):

$$L_{wire} = \frac{L_{Cable}}{L_{Pitch}} \sqrt{L_{Pitch}^2 + \pi^2 D^2} \tag{10}$$

B. DC AND AC RESISTANCES

As discussed in the previous section, two resistive components are needed to model resistance of the transmission line due to redistribution of the current in the cross-sectional area of a conductor by altering the operating frequency. One component to model DC resistance and the other for modeling AC resistance of the conductor. The DC resistance is simply calculated according to simple resistivity equation as follows:

$$R_{DC} = \rho \frac{4l}{\pi d^2} \tag{11}$$

where ρ is the specific electrical resistance of the copper. Hence the DC resistance matrix comes in the form of (12):

$$R_0 = \begin{bmatrix} \rho \frac{4l}{\pi d^2} & 0 \\ 0 & \rho \frac{4l}{\pi d^2} \end{bmatrix} \tag{12}$$

At DC frequencies, the current distribution in a conductor is uniform in the cross sectional area. By increasing the frequency, the magnetic field within the conductor forces the current to flow from the lower impedance paths closer to the surface of the conductor. This mechanism which increases the apparent resistance of the wire is called skin effect and can be represented by diagonal elements in the AC resistance matrix.

Although the current density drops off exponentially from the surface towards the center of the conductor (Fig. 6(a)), for easing mathematical calculations, it is assumed that the whole of the current only follows in a shallow region near the surface (Fig. 6(b)). The thickness of this region which is defined as skin depth and announced by δ is determined based on the point at which the current density falls to 37 percent of its value near the surface [1].

The general formula for the skin depth is given in (13):

$$\delta = \sqrt{\frac{\rho}{\pi f \mu_0 \mu_r}} \tag{13}$$

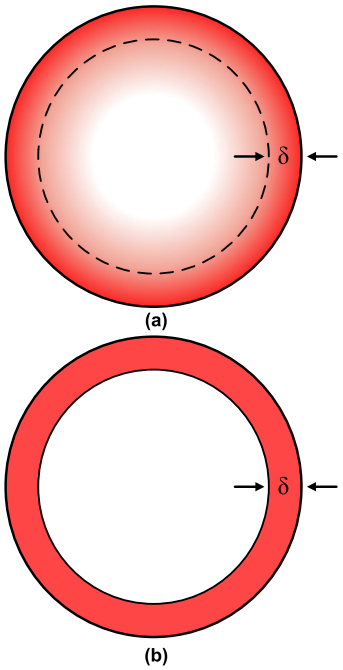

FIGURE 6. (a) Real (b) approximate current distribution profile in cross sectional area of a rod wire at some frequency.

where f, μ_0 and μr are transmitted signal frequency, the magnetic permeability of the free space and relative magnetic permeability of conductor, respectively. As is clear, the skin depth depends on the electrical and magnetic characteristics of the conductor in addition to the frequency of the signal which is transmitted through it. By substituting the effective cross-sectional area of the conductor that is shown in Fig. 6(b) in (11), AC resistance of the conductor is obtained as (14):

$$\mathrm{R_{AC}\,(f)} = \rho \frac{l}{\pi \mathrm{d}\delta - \pi \delta^2} \tag{14}$$

Since the skin depth is much smaller than the diameter of the wire, the second-order term in (14) can be neglected. By doing so and replacing δ according to the (13), the following equation is obtained based on the (15) [5]:

$$\mathrm{R_{AC}\,(f)} \cong \frac{l}{\mathrm{d}} \sqrt{\frac{\mathrm{f}\mu_0\mu_\mathrm{r}\rho}{\pi}} \tag{15}$$

When an AC flows through two nearby conductors, proximity effect is the other phenomenon that causes their apparent resistance to seem greater than the value that is expected from the skin effect alone [39], [40]. The current distribution of adjacent wires with the same and opposite direction current flows is illustrated in Fig. 7(a) and (b), respectively.

Although the varying magnetic field of the adjacent conductor [42] perturbs the redistribution of the current around the perimeter of the wire and must be modeled in terms of the off-diagonal elements in AC resistance matrix, it is possible to conceptually consider that the proximity effect leads to increase the skin effect due to further current crowding [8].

Hence, the impact of the proximity effect can be intervened in (15) by correction factor $\mathrm{k_p}$ [30] as (16) implies. The

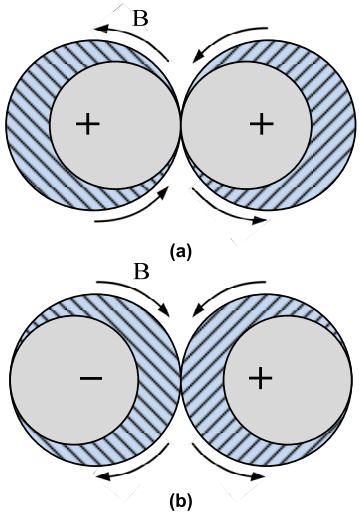

FIGURE 7. Proximity effect in two parallel round wire with current following in (a) same (b) opposite direction.

magnitude of this factor is determined by the ratio of the wire separation and its diameter [28]. Based on the characteristics that are available from the cable vendor, this ratio is equal to 1.78 for the twisted pair cable which is selected as a case study in this paper. Thus, the value of the proximity effect correction factor will be 1.2 according to [43].

$$\mathrm{R_{AC}\,(f)} \cong \mathrm{k_p} \frac{l}{\mathrm{d}} \sqrt{\frac{\mathrm{f}\mu_0\mu_\mathrm{r}\rho}{\pi}} \tag{16}$$

By inspecting (16), AC resistance of the conductors is proportional to the square root of the frequency. Therefore, the AC resistance matrix of the W-element comes in the following form:

$$\mathrm{R_S} = \begin{bmatrix} \mathrm{k_p} \frac{l}{\mathrm{d}} \sqrt{\frac{\mu_0\mu_\mathrm{r}\rho}{\pi}} & 0 \\ 0 & \mathrm{k_p} \frac{l}{\mathrm{d}} \sqrt{\frac{\mu_0\mu_\mathrm{r}\rho}{\pi}} \end{bmatrix} \tag{17}$$

C. SELF AND MUTUAL INDUCTANCES

It is well known that a current carrying conductor is surrounded by concentric magnetic flux lines. In the case of alternative current being transmitted, this variation of magnetic flux induces a voltage. This phenomenon which poses a resistance against the current flow can be modeled as an inductance. When two conductors are placed very close to each other like balanced transmission lines, the current of one conductor affects the magnetic flux of the other one. So both self and mutual inductance of the wires should be considered to calculate the total inductance of the transmission line. Self and mutual inductance of the parallel wires can be obtained according to the (18) and (19) [44].

$$\mathrm{L_S} = 2\left[l\mathrm{Ln}\left(\frac{2l + \sqrt{4l^2 + \mathrm{d}^2}}{\mathrm{d}} \right) - \frac{\sqrt{4l^2 + \mathrm{d}^2}}{2} \right] \tag{18}$$

$$M = 2\left[l\mathrm{Ln}\left(\frac{l+\sqrt{l^2+D^2}}{D}\right)-\sqrt{l^2+D^2}\right] \quad (19)$$

Since current flows in opposite direction in two wires of the twisted pair cable, so the total inductance is calculated as (20):

$$L = 2L_s - 2M \quad (20)$$

D. DIELECTRIC LOSS

The frequency-dependent characteristics of the dielectric loss originate from the fact that how much dipoles of the insulation material are able to move by increasing frequency [33]. This effect is characterized by the dissipation factor, namely tan(δ), which is equal to the tangent of the angle between real and imaginary parts of the electrical permittivity. The value of the dielectric loss of the insulation material at a specified frequency is obtained by (21) [45]:

$$G(f) = \frac{2\pi^2 l f \varepsilon_0 \varepsilon_r \tan\delta}{\mathrm{Ln}(\frac{D}{d}+\sqrt{(\frac{D}{d})^2-1})} \quad (21)$$

As is clear dielectric loss depends on the wire's geometry in addition to the loss tangent and frequency. Since G(f) is directly proportional to the operating frequency, so G_{dm} comes in the following form based on the (22).

$$G_{dM} = \frac{2\pi^2 l \varepsilon_0 \varepsilon_r \tan\delta}{\mathrm{Ln}(\frac{D}{d}+\sqrt{(\frac{D}{d})^2-1})} \quad (22)$$

According to the all above discussions, the AC dielectric loss matrix can be written as (23):

$$G_d = \begin{bmatrix} \frac{2\pi^2 l \varepsilon_0 \varepsilon_r \tan\delta}{\mathrm{Ln}(\frac{D}{d}+\sqrt{(\frac{D}{d})^2-1}))} & -\frac{2\pi^2 l \varepsilon_0 \varepsilon_r \tan\delta}{\mathrm{Ln}(\frac{2D}{d})} \\ -\frac{2\pi^2 l \varepsilon_0 \varepsilon_r \tan\delta}{\mathrm{Ln}(\frac{2D}{d})} & \frac{2\pi^2 l \varepsilon_0 \varepsilon_r \tan\delta}{\mathrm{Ln}(\frac{2D}{d})} \end{bmatrix} \quad (23)$$

E. SELF AND MUTUAL CAPACITANCE

It is obvious that there is some mutual capacitance between the conductors of the transmission line due to the potential difference between them [8]. Conductors and their insulation material act as plates and dielectric of this capacitance, respectively. (24) shows the dependency of the mutual capacitance to the wire's geometries [46]:

$$C_M = \frac{\pi \varepsilon_0 \varepsilon_r l}{\mathrm{Ln}(\frac{D}{d}+\sqrt{(\frac{D}{d})^2-1})} \quad (24)$$

where ε_0 and ε_r are the vacuum permittivity and relative permittivity of insulation material, sequentially. As is clear, this equation is proportional to the length of the transmission line.

The self-capacitor of twisted pair wires has two dielectric media in series between its plates with different permittivity coefficients. In fact, this capacitor is a series equivalent of two capacitors whose dielectric media is insulation media of conductors and air. Since the size of the capacitor with air dielectric is much smaller than the other capacitor, so the value of self-capacitance is approximately equal to it. Consequently, to evaluate the self-capacitance of the wires with respect to the ground, it is enough to calculate the capacitance of a straight horizontal rod which is elevated at a height h, above the earth as shown in Fig. 8 [47].

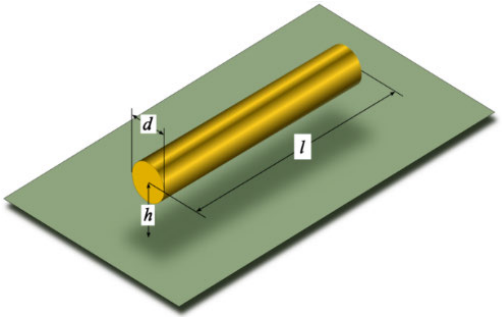

FIGURE 8. An elevated round wire at height of h.

To find an exact and absolute model for the capacitor of the twisted pair cable, different factors such as excitation mode, frequency, cable's type and earth electrical properties must be taken into account carefully regardless of their effect rate. Since the main purpose of this work is to provide a simple and straightforward method of modelling with acceptable accuracy, some assumptions are made. As the twisted pair cables are not buried underground and usually are installed inside the PVC trunks at a specific height above the earth, so the earth can be considered as perfect ground plane to calculate self-capacitance. To be more cautious, the thickness of the cables insulation material and its permittivity should be involved in this equation. But as the thickness of the insulation is negligible with respect to the installation height, it can be ignored to keep the method as straightforward as possible.

Based on the mentioned points, (25) indicates the equation of the self-capacitance:

$$C_S = \frac{2\pi \varepsilon_0 l}{\mathrm{Ln}(\frac{2h}{d}+\sqrt{(\frac{2h}{d})^2-1})} \quad (25)$$

As $h \gg d$, (25) can be approximated as follows:

$$C_S = \frac{2\pi \varepsilon_0 l}{\mathrm{Ln}(\frac{4h}{d})} \quad (26)$$

It is obvious that the parameters of the W-element model for twisted pair cable can be easily and directly obtained by placing the value of the cable characteristics according to the datasheet in the proposed formulas, without any excessive effort and time-wasting. On the contrary, for extracting the cable's parameters in the conventional methodologies that rely on S-parameter or time-domain measurements, all measurements or simulation steps must be repeated if even only

one of the cable's parameters changes. This issue is very important from the complexity analysis point of view. Indeed, the complexity and amount of the time and effort needed to extract the parameters of a model are the key factors to assess its performance. Big-O notation is a common mathematical notation used for this purpose. The letter O is used because the growth rate of a function is also referred to as the order of the function. The fastest possible running time for any algorithm is O(1), commonly referred to as constant running time. O(n), $O(n^2)$, $O(n^3)$, etc. is utilized for describing the complexity of the more complicated algorithms. As the proposed methodology always takes the same amount of time to execute, it can be considered as an algorithm with O(1) complexity degree.

V. EVALUATION OF W-ELEMENT MODEL FOR A TYPICAL TWISTED PAIR CABLE

Since unshielded CAT6 twisted pair cable is the best candidate for the most of today's networks by taking into account it's all pros and cons, W-element model of this type of twisted pair cable is extracted in this section to evaluate the validity of the formulas by comparing its accuracy and performance against real Fluke test results and HFSS simulations. For this purpose, LANmark-6 U/UTP Cable of Nexans S.A. Company with part number of N100.607 is selected as a case study [48]. It is worth noting that this company is the world's second largest manufacturer of cables. A list of the main characteristics of the aforesaid cable type is gathered in Table 1.

TABLE 1. NEXANS N100-607 CAT 6 twisted pair cable characteristics.

Part number	N100.607
Model name	LANmark-6
Category	Cat. 6
Type of cable	U/UTP
Outer sheath	LSZH
Screen	Unshielded
Diameter over insulation (D)	1.02 mm
Conductor cross-section (d)	23 AWG (0.5733 mm)
Nominal outer diameter	6.3 mm
Mutual capacitance	56 nF/km
Characteristic impedance (Z0)	100 Ohm
NVP	69%

Assuming that the rise time is 150 ps for 0.35μm CMOS technology and NVP of the cable is 69%, the maximum allowable length that could be considered as a lumped element would be 6 mm. Hence, 2 mm is an appropriate choice for the length of each lumped element by aforesaid assumptions. W-element matrices of the 2 mm unit length of the wire are calculated as follows:

$$R_0 = \begin{bmatrix} 133.3 & 0 \\ 0 & 133.3 \end{bmatrix} \times 10^{-6} \quad (27)$$

$$R_S = \begin{bmatrix} 3.76 & 0 \\ 0 & 3.76 \end{bmatrix} \times 10^{-7} \quad (28)$$

$$L_0 = \begin{bmatrix} 6.52 & 1.21 \\ 1.21 & 6.52 \end{bmatrix} \times 10^{-10} \quad (29)$$

$$C = \begin{bmatrix} 9.52 & -8.38 \\ -8.38 & 9.52 \end{bmatrix} \times 10^{-14} \quad (30)$$

$$G_0 = 0 \quad (31)$$

$$G_d = \begin{bmatrix} 1.05 & -1.05 \\ -1.05 & 1.05 \end{bmatrix} \times 10^{-16} \quad (32)$$

A. VALIDATION OF THE PROPOSED W-ELEMENT MODEL

Unlike straightforward installation procedure of the twisted pair cable, evaluating circuit equivalent and certifying it is not very convenient anymore. Almost in all network projects, the Fluke test is used as a qualifying tool to validate the performance of the cabling infrastructure. To the author's best knowledge, Fluke Corporation is one of the world leaders in the manufacturing, distribution and service of electronic test equipment. Thus, the fluke test can be considered as an appropriate criteria for evaluating the accuracy of the extracted W-element model. In this paper, a data set of 1000 channel type Fluke test results is exploited for this purpose. All of these tests have been done with the Fluke DTX-1800 cable analyzer. Fig. 9 illustrates a typical twisted pair cable test that is done with this device.

FIGURE 9. Typical twisted pair cable testing with Fluke DTX-1800 cable analyzer.

When using a cable certifier, it is important to pay attention to the type of test which is set on the device. Permanent link and channel type is the more common test types of the Fluke cable testing procedure. Fig. 10 reveals the difference between the permanent link and channel test types. In the permanent link test type, only cabling from the patch panel to the work area outlet and connectors are considered. Alternatively, whole connections between a network device (such as switch or router) and endpoint PC which consist of permanent link, patch cords and RJ45 connectors [49], [50] are included in the channel test. In both cases, total loss of two RJ45 connectors must be subtracted from the results to fairly judge the net loss which only corresponds to the twisted pair cable itself. It should be bear in mind that the loss value that manufacturers provide for their connectors is based on the factory tests in which they are mated to high-quality reference connectors.

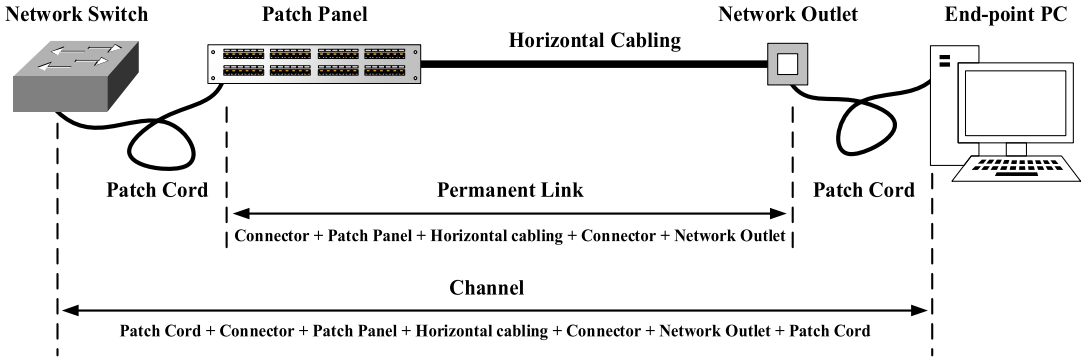

FIGURE 10. Permanent link versus channel link.

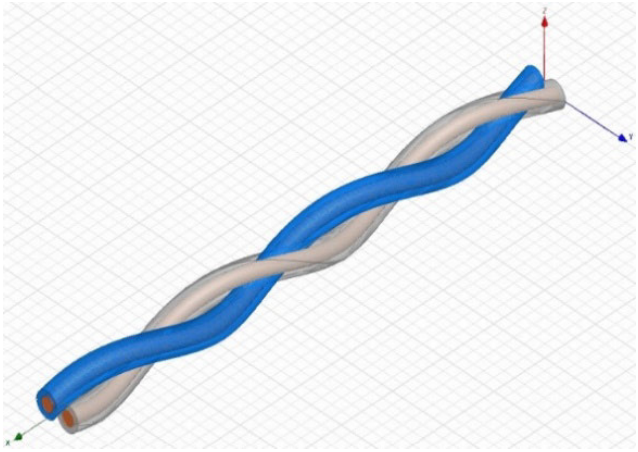

FIGURE 11. Designed twisted pair cable by HFSS software.

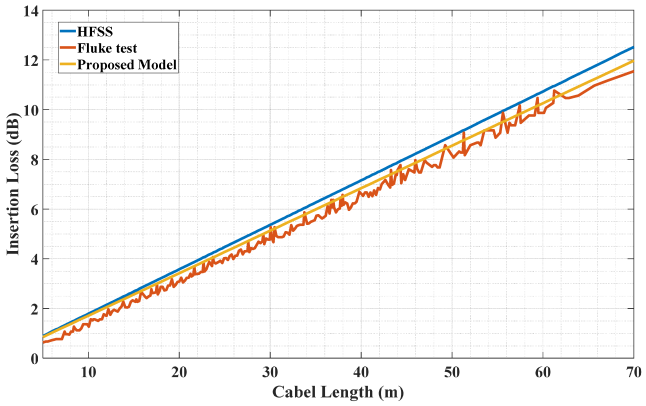

FIGURE 12. Insertion loss vs. cable length @ 100 MHz.

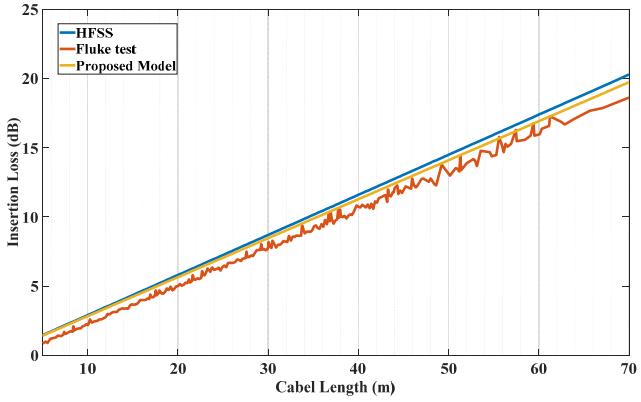

FIGURE 13. Insertion loss vs. cable length @ 250 MHz.

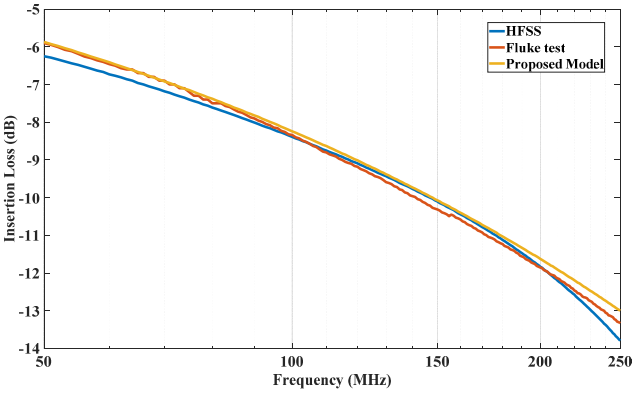

FIGURE 14. Insertion loss vs. frequency (logarithmic scale) @ 50 meters cable length.

As this issue does not fully fulfill most practical cases and the maximum allowed insertion loss for a typical connector based on the TIA standards recommendation is 0.75 dB, any value between 0.2 dB and 0.7 dB can be expected for insertion loss of each connector that its Fluke test is passed. This ambiguity is one the sources of the error between the extracted model and Fluke test results. In addition to connectors, the insertion loss of cable and patch cord should be studied individually to be more cautious in the case of channel test type.

Besides the fluke tester, HFSS simulation is carried out to further assess the performance of the derived model. This software is a versatile electromagnetic field simulator that is suitable for analyzing any arbitrary 2D/3D forms of electronic devices such as antennas, high-speed interconnects and etc.

Insertion loss is one of the key parameters used to analyze the performance and quality of the inserted component in telecommunication. Accordingly, the amount of the insertion loss of the derived model is compared with respect to those power loss values that are obtained by the Fluke test and HFSS simulation runs. As the amount of cable insertion

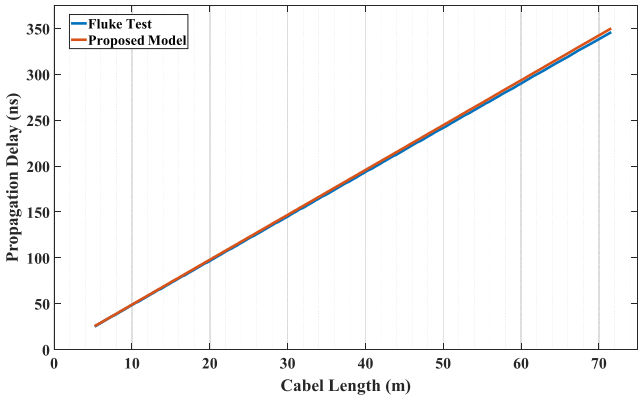

FIGURE 15. Propagation delay vs. cable length.

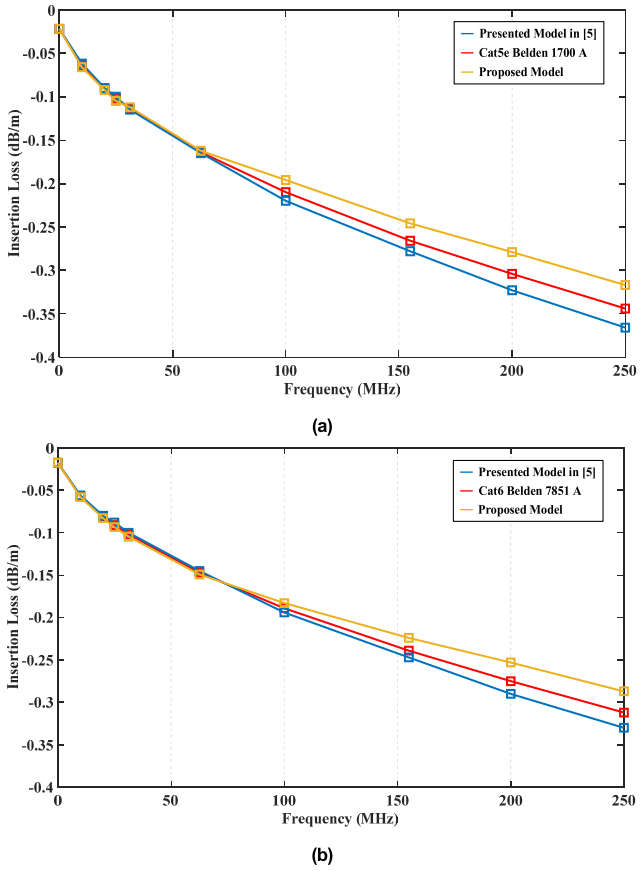

FIGURE 16. Comparison of the proposed method and the one presented in [5].

loss increases by increasing the frequency and cable length, separate comparisons are made to assess the dependencies of these factors, as shown in Fig. 12 to Fig. 14. Comparative results confirm the accuracy of the derived W-element for the Cat 6 twisted pair cable which is selected as a case study.

Propagation delay or the amount of the time required for a signal to propagate from one end of the transmission line to the other end, is another important parameter for evaluating the performance of the network cables. The propagation delay in a twisted-pair cable is related to the nominal velocity of propagation (NVP) and its length. The value of NVP is

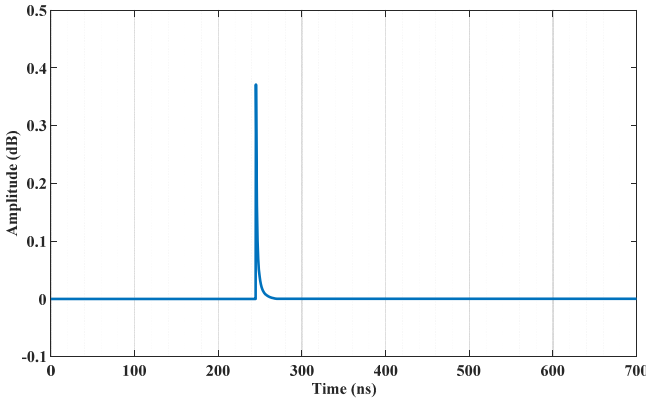

FIGURE 17. Impulse response of the proposed W-element model.

specified by cable vendors as a percentage that indicates the speed of signal traveling in the cable relative to the speed of the light in vacuum. Since the propagation delay changes with frequency, so it is obvious that the value of NVP is not constant along the frequency range. Therefore, ANSI/TIA-1152 standards state that measurement for propagation delay and NVP has to be done at 10 MHz. Additionally, NVP is defined according to the pair with the longest twist length which has the shortest electrical delay. Fig. 15 illustrates a comparison between the propagation delay of the real FLUKE test and the extracted W-element model. This results proves the correctness of the proposed model. The maximum difference between the proposed model and the Fluke test is about 1.7 % which is tolerable for the rule of thumb analysis.

For further performance assessment, the validity of the proposed methodology is compared to the results provided in [5]. In that paper, two different types of twisted pair cables, namely Cat5e Belden 1700A and Cat6 Belden 7851A, are modeled based on the time domain measurements. The aforesaid cables' W-element model is extracted using the proposed methodology, and the comparison is made based on the insertion loss (attenuation) of the models. Fig. 16 illustrates the comparison results between these models and proofs the validity of the proposed method.

Although the model introduced in [5] is a bit more accurate than the model proposed in this paper, but it needs time wasting TDR measurements for each frequency point. This overwhelming approach increases the complexity of the modeling. While the proposed method in this paper is more straightforward to use and can be considered as a good engineering procedure to obtain rapid insights about the performance of the twisted pair cables.

The causality is another important characteristic when considering the time-domain representation of a model [27]. The causality of the model can be interpreted from the impulse response which is derived by the inverse Fourier transform of the frequency response. In a non-casual model, the impulse response has significant energy during the propagation delay [51]. Fig. 17 depicts the impulse response of the 50 meters of the selected cable as a case study. The propagation delay

of the mentioned length of the cable is 244.5 ns. The result reveals the causality of the derived model.

VI. CONCLUSION

It can be concluded that in opposition to the simple installation mechanism of the twisted pair cable, evaluating a circuit equivalent for twisted pair cable and certifying it is not very convenient anymore. So in this paper, a set of closed-form equations and W-element model were proposed for straightforward modeling of the twisted pair cables based on their structural and electrical characteristics. Unlike the time consuming and tedious procedure of using the field solver software such as ANSYS Maxwell or HFSS for investigating the performance of the cable, the proposed model can be exploited by both system designers and cable manufacturers to gain rapid and clear insight into the overall behavior of the balanced transmission lines prior to fabrication. Scrutinizing the effect of each individual parameter is easily possible by this model. It is enough to place new value in the proposed equations to obtain the results. Since the algorithm of W-element does not have any hard frequency limitations, so the derived model can be exploited for almost all operating frequency ranges of the cables. The proposed model can be applicable to extract the parameters of the variety of cable types in which each case is an interesting topic for future works. As Nexans unshielded CAT6 twisted pair cable is one of the most common types of used cables in today's networks, it was selected as a case study in this paper for verification of the proposed model. Diversity of the simulations and comparisons have been performed to evaluate the validity of the provided model. Additionally, the performance of the model is assessed in regard to the real Fluke test results. Furthermore, performance of the proposed method is evaluated regarding to the results provided for two other twisted pair cables, namely Cat5e Belden 1700A and Cat6 Belden 7851A that are reported in the literature.

REFERENCES

[1] J. J. Yoho, "Physically-based realizable modeling and network synthesis of subscriber loops utilized in DSL technology," Ph.D. dissertation, Virginia Tech, Blacksburg, VA, USA, 2001.

[2] W. Fang, Y. Ren, X. Liu, X. Jiao, and C. Chu, "Parameter extraction method for the twisted pair cable with rectangular connectors," *PLoS ONE*, vol. 13, no. 10, Oct. 2018, Art. no. e0205072.

[3] B. C. Wadell, *Transmission Line Design Handbook*. Norwood, MA, USA: Artech House, 1991.

[4] M. J. Degerstrom, B. K. Gilbert, and E. S. Daniel, "Accurate resistance, inductance, capacitance, and conductance (RLCG) from uniform transmission line measurements," in *Proc. IEEE-EPEP Electr. Perform. Electron. Packag.*, Oct. 2008, pp. 77–80.

[5] D. Gilsic, "LVDS pre-emphasis boosts cable performance," Nat. Semicond. Company, Texas Instrum., Dallas, TX, USA, Tech. Rep., 2005.

[6] W. Ben Hassen, M. Kafal, and E. Cabanillas, "A stranded unshielded twisted pair modeling for online fault location using OMTDR-based diagnosis sensor," in *Proc. 8th Int. Conf. Sensor Netw.*, 2019, pp. 40–46.

[7] J. M. Rabaey, A. P. Chandrakasan, and B. Nikolic. *Digital Integrated Circuits: A Design Perspective*. vol. 7. Upper Saddle River, NJ, USA: Pearson Education, 2003.

[8] E. Bogatin, *Signal and Power Integrity-Simplified*. Upper Saddle River, NJ, USA: Prentice-Hall Professional, 2004.

[9] M. M. Al-Asadi, A. P. Duffy, K. G. Hodge, A. J. Willis, "Twisted pair cable design analysis and simulation," in *Proc. 49th Int. Wire Cable Symp. (IWCS)*, 2000, pp. 111–120.

[10] D. M. Pozar, *Microwave Engineering*. Hoboken, NJ, USA: Wiley, 2009.

[11] A. Asrokin, M. K. A. Rahim, A. N. Z. Abidin, N. Hashim, and S. A. Azis, "Cable modelling comparison for twisted-pair copper plant in Malaysia," in *Proc. IEEE Int. Conf. Control Syst., Comput. Eng. (ICCSCE)*, Nov. 2015, pp. 359–364.

[12] R. Papazyan, P. Pettersson, H. Edin, R. Eriksson, and U. Gafvert, "Extraction of high frequency power cable characteristics from S-parameter measurements," *IEEE Trans. Dielectr. Electr. Insul.*, vol. 11, no. 3, pp. 461–470, Jun. 2004.

[13] S. B. Goldberg, M. B. Steer, P. D. Franzon, and J. S. Kasten, "Experimental electrical characterization of interconnects and discontinuities in high-speed digital systems," *IEEE Trans. Compon., Hybrids, Manuf. Technol.*, vol. 14, no. 4, pp. 761–765, Dec. 1991.

[14] D. F. Williams, J. E. Rogers, and C. L. Holloway, "Multiconductor transmission-line characterization: Representations, approximations, and accuracy," *IEEE Trans. Microw. Theory Techn.*, vol. 47, no. 4, pp. 403–409, Apr. 1999.

[15] G. Chen, L. Zhu, and K. L. Melde, "Extraction of frequency dependent RLCG parameters of the packaging interconnects on low-loss substrates from frequency domain measurements," in *Proc. IEEE 14th Topical Meeting Electr. Perform. Electron. Packag.*, Oct. 2005, pp. 25–28.

[16] J.-H. Kim and D.-H. Han, "Hybrid method for frequency-dependent lossy coupled transmission line characterization and modeling," in *Proc. Electr. Perform. Electr. Packag.*, Oct. 2003, pp. 239–242.

[17] A. Deutsch, G. Arjavalingam, and G. V. Kopcsay, "Characterization of resistive transmission lines by short-pulse propagation," *IEEE Microw. Guided Wave Lett.*, vol. 2, no. 1, pp. 25–27, Jan. 1992.

[18] P. Ferrari, B. Flechet, and G. Angenieux, "Time domain characterization of lossy arbitrary characteristic impedance transmission lines," *IEEE Microw. Guided Wave Lett.*, vol. 4, no. 6, pp. 177–179, Jun. 1994.

[19] W. Kim, S. Hee Lee, M. Cheol Seo, M. Swaminathan, and R. R. Tummala, "Determination of propagation constants of transmission lines using 1-port TDR measurements," in *59th ARFTG Conf. Dig. Spring*, Jun. 2002, p. 6.

[20] D. Jaisson, "Simple time-domain model for a shielded twisted pair of wires," *IEEE Trans. Electromagn. Compat.*, vol. 58, no. 4, pp. 1151–1157, Aug. 2016.

[21] B. Milovanovic, A. Marincic, and N. Dončov, "Characterization of twisted pair telephone cable for broadband telecommunication services," in *Proc. 23rd POSTEL Symp., Fac. Traffic Transp. Eng.*, Beograd, Serbia, 2005, pp. 241–251.

[22] M. Timmers, M. Guenach, C. Nuzman, and J. Maes, "G.Fast: Evolving the copper access network," *IEEE Commun. Mag.*, vol. 51, no. 8, pp. 74–79, Aug. 2013.

[23] R. Van Den Brink and B. Van Den Heuvel, "G. fast: Wideband modeling of twisted pair cables as two-ports," Standard 11GS3-028, ITU-T SG15 Q4 Contrib., 2011.

[24] G. Shirkoohi, "Modelling and simulation of fault detection in shielded twisted pair cables," in *Proc. IEEE Int. Conf. Ind. Technol. (ICIT)*, Mar. 2016, pp. 1039–1044.

[25] J. E. Miller, "Numerical modeling of impacts of twisted-pair data cables," in *Proc. Hypervelocity Impact Symp.* New York, NY, USA: American Society Mechanical Engineers, vol. 883556, 2019, Art. no. V001T10A006.

[26] J. Zhang, J. L. Drewniak, D. J. Pommerenke, M. Y. Koledintseva, R. E. DuBroff, W. Cheng, Z. Yang, Q. B. Chen, and A. Orlandi, "Causal RLGC (f) models for transmission lines from measured S-parameters," *IEEE Trans. Electromagn. Compat.*, vol. 52, no. 1, pp. 189–198, Feb. 2010.

[27] D. Acatauassu, S. Höst, C. Lu, M. Berg, A. Klautau, and P. O. Börjesson, "Simple and causal twisted-pair channel models for G.Fast systems," in *Proc. IEEE Global Commun. Conf. (GLOBECOM)*, Dec. 2013, pp. 2834–2839.

[28] T. K. Truong, "Twisted-pair transmission-line distributed parameters," in *Proc. EDN Mag.*, 2000.

[29] O. E. Ogundapo, "High frequency Ethernet cabling analysis and optimization," Ph.D. dissertation, De Montfort Univ., Leicester, U.K., 2016.

[30] H. Johnson, H. W. Johnson, and M. Graham, *High-Speed Signal Propagation: Advanced Black Magic*. Upper Saddle River, NJ, USA: Prentice-Hall Professional, 2003.

[31] *HSPICE User Guide: Signal Integrity, Version E-2010.12*, Synopsys, Mountain View, CA, USA, Dec. 2010.

[32] *Star-Hspice Manual, Avant! Corporation and Avant! Subsidiary, Release 1998.2*, Synopsys Company, Research Triangle, NC, USA, Jul. 1998.

[33] T. C. Edwards and M. B. Steer, *Foundations of Interconnect and Microstrip Design*. New York, NY, USA: Wiley, 2000.
[34] B. J. Elliott, *Cable Engineering for Local Area Networks*. Boca Raton, FL, USA: CRC Press, 2000.
[35] A. Bouchaala, L. Courau, O. Bonnaud, and P. Galy, "W-element RLGC matrices calculation for power distribution planes modeling using MCTL matrix method," *IEEE Electromagn. Compat. Mag.*, vol. 5, no. 3, pp. 61–69, 3rd Quart., 2016.
[36] E. D. Lorenzo. (2011). *The Maxwell Capacitance Matrix*. [Online]. Available: http//www.fastfieldsolver.com
[37] *Commercial Building Telecommunications Cabling Standard Part 2: Balanced Twisted-Pair Cabling Components Revision Of TIA*, Standard TIA, EIA EIA-568-B. 2, Rev. B, 2001, pp. 1–11.
[38] E. Wasserman and D. Neilson, "Applied wave research's analog office extends HSPICE transient simulations to RF frequencies," AWR Inc, Tulalip, WA, USA, 2003.
[39] W. L. Stutzman and G. A. Thiele. *Antenna Theory and Design*. Hoboken, NJ, USA: Wiley, 2012.
[40] K. Ferkal, M. Poloujadoff, and E. Dorison, "Proximity effect and eddy current losses in insulated cables," *IEEE Trans. Power Del.*, vol. 11, no. 3, pp. 1171–1178, Jul. 1996.
[41] G. Smith, "The proximity effect in systems of parallel conductors and electrically small multiturn loop antennas," Dept. Division Eng. Appl. Phys., Harvard Univ., Cambridge, MA, USA, Tech. Rep. TR-624, 1971.
[42] M. K. Kazimierczuk, *High-Frequency Magnetic Components*. Hoboken, NJ, USA: Wiley, 2009.
[43] F. E. Terman, *Radio Engineers' Handbook*. New York, NY, USA: McGraw-Hill, 1943.
[44] E. B. Rosa, *The Self and Mutual Inductances of Linear Conductors*, Standard 80, U.S. Department of Commerce and Labor, Bureau of Standards, 1908.
[45] A. V. Vorst, A. Rosen, and Y. Kotsuka, *RF/Microwave Interaction With Biological Tissues*, vol. 181. Hoboken, NJ, USA: Wiley, 2006.
[46] S. Ramo, J. R. Whinnery, and T. Van Duzer. *Fields and Waves in Communication Electronics*. Hoboken, NJ, USA: Wiley, 1994.
[47] E. C. Jordan and G. K. Balmain, *Electromagnetic Waves and Radiating Systems*, 2nd ed. Upper Saddle River, NJ, USA: Prentice-Hall, 1968.
[48] *LANmark-6 U/UTP AWG23 Cat 6 350MHz LSZH Eca Orange 305m Box*, document N100-607, NEXANS Company, 2020.
[49] *LANmark-6 Patch Cord Cat 6 Unscreened LSZH 1m Orange*, document N116.P1A010OK, NEXANS Company, 2020.
[50] *LANmark-6 Evo Snap-In Connector Category 6 Unscreened*, document N420.660, NEXANS Company, 2020.
[51] D. Acatauassu, S. Host, C. Lu, M. Berg, A. Klautau, and P. O. Borjesson, "Simple and causal copper cable model suitable for G.Fast frequencies," *IEEE Trans. Commun.*, vol. 62, no. 11, pp. 4040–4051, Nov. 2014.

MOHAMMAD ZAREI (Member, IEEE) was born in Urmia, Iran, in 1987. He received the B.S. and M.Sc. degrees in electrical engineering from Urmia University, Urmia, in 2009 and 2012, respectively, where he is currently pursuing the Ph.D. degree in electrical engineering. His research interests are analog and digital integrated circuit design, computer networks, fuzzy systems, and neural networks.

AMIN KHALILZADEGAN (Member, IEEE) was born in Urmia, Iran, in 1987. He received the B.S. (Hons.) and M.Sc. (Hons.) degrees in electrical engineering from Urmia University, Urmia, in 2009 and 2012, respectively, where he is currently pursuing the Ph.D. degree in electrical engineering. His research interests are analog and digital integrated circuit design, computer networks, fuzzy systems, and neural networks.

KHAYROLLAH HADIDI (Member, IEEE) received the B.S. degree from the Sharif University of Technology, Tehran, Iran, the M.S. degree from Polytechnic University, New York, and the Ph.D. degree from the University of California, Los Angeles, all in electrical engineering. He is currently with the Electrical Engineering Department and Microelectronics Research Laboratory at Urmia University, Urmia, Iran. He holds four U.S., U.K., and German patents (issued), plus 12 Japanese patents (pending). His research interests are high-speed high-resolution data converter design, wideband integrated filter design, and nonlinearity analysis and improvement in analog circuits.